UNITED
NATIONS

E

Economic and Social
Council

Distr.
GENERAL

ECE/EB.AIR/WG.1/2008/8
9 July 2008

Original: ENGLISH

ECONOMIC COMMISSION FOR EUROPE

EXECUTIVE BODY FOR THE CONVENTION ON LONG-RANGE
TRANSBOUNDARY AIR POLLUTION

Working Group on Effects

Twenty-seventh session
Geneva, 24–26 September 2008
Item 4 of the provisional agenda

RECENT RESULTS AND UPDATING OF SCIENTIFIC AND TECHNICAL KNOWLEDGE

COMBINED EFFECTS OF CLIMATE CHANGE AND AIR POLLUTION ON MATERIALS INCLUDING CULTURAL HERITAGE

Report by the Programme Centre of the International Cooperative Programme on Effects of Air Pollution on Materials, including Historic and Cultural Monuments

INTRODUCTION

1. Climate change is currently attracting a lot of interest at both the research and policy levels. However, the degradation of materials and cultural heritage caused by climate change has not yet been addressed in international programmes and has so far not received less focus than other effects of climate change. This report summarizes the use of dose-response functions for

corrosion from ICP Materials[1] in a recently concluded European Union (EU) project "Global Climate Change Impact on Built Heritage and Cultural Landscapes" (NOAHs ARK). After a general introduction, particular emphasis will be given on results on combined effects of climate change and air pollution. A key element of the NOAHs ARK project has been the use of dose-response and damage functions in order to predict the possible impact of future climate change based on different scenarios. Further information is available at: http://noahsark.isac.cnr.it/. The main results are presented here in accordance with item 3.2 of the 2008 workplan for the implementation of the Convention (ECE/EB.AIR/91/Add.2) adopted by the Executive Body at its twenty-fifth session.

I. CLIMATE MODELS AND EMISSION SCENARIOS

2. Climatic parameters were extracted from a general climate model (HadCM3) and a regional climate model (HadRM3) of the Hadley Centre in the United Kingdom. The general model has a grid resolution of 2.5º × 3.75º, which corresponds to about 300 km × 300 km at 45º northern latitude (figure 1). The regional model has a higher resolution of 50 km × 50 km.

3. Only one scenario has been considered, the A2 scenario of the Intergovernmental Panel on Climate Change. In this scenario, the economic development is primarily regional in orientation and per capita economic growth and technological change is relatively more fragmented and slower compared to other scenarios.

4. The selected geographical area is centred on Europe (figure 1). The general HadCM3 model has generated data with seasonal and yearly resolutions for three periods. They are denoted as "recent past" (1961–1990), "near future" (2010–2030) and "far future" (2070–2099). The regional HadRM3 model has generated data only for the far future period.

5. Data generated from the models include temperature range, thermal shocks (>7, >10, >15 and >20°C), mean temperature, freeze-thaw cycles, frost damage, total rain days, rainy periods (1, 2, 3, 4, 5, 6, 7, 8, 9 and ≥10 days), extreme rain (>20 mm/day), total precipitation amount, relative humidity range, mean relative humidity, relative humidity cycles, relative humidity shocks, wind speed, extreme wind (>7.5, >10, >15 and >20 m/s) and wind-driven rain. These are the most important climatic parameters that individually or in combination with other parameters can have an effect on degradation of heritage materials.

[1] The International Cooperative Programme on Effects of Air Pollution on Materials, including Historic and Cultural Monuments.

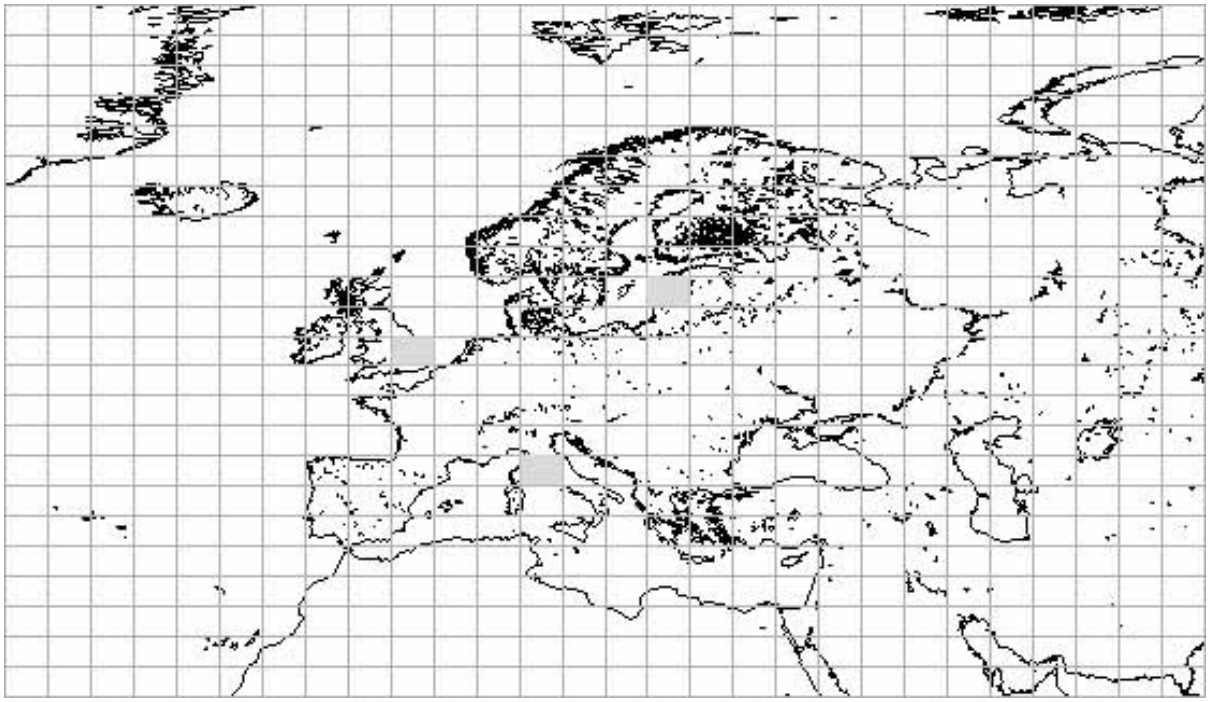

Figure 1. Selected geographical area and grid for the general climate model HadCM3. Three grid cells have been marked: “Riga”, “London” and “Rome”.

II. VULNERABILITY ATLAS

6. The map section of the vulnerability atlas consist of one map for the regional model (2070–2099), three maps for the general climate model (1961–1990, 2010–2030 and 2070–2099) and two difference maps for the general climate model (2010-2030 compared to 1961–1990 and 2070–2099 compared to 1961–1990). Map pages are classified as climate maps, heritage climate maps, damage maps, risk maps and multiple-risk maps.

7. Heritage climate maps are obtained by combining climate parameters, with the aim of constructing factors believed to be especially important for the degradation of cultural heritage. They comprise salt crystallization, wet-frost, biomass accumulation of monuments and lichen species richness.

8. Damage maps are specific to a material or group of material and are based on dose-response or damage functions for those materials. They include surface recession of low porous carbonate stones, thermoclastism (microcracking of stone materials caused by repeated thermally induced expansion and contraction), climate-induced decay of clay containing materials, steel-iron and bronze corrosion caused by acidifying pollutants in urban areas, zinc (Zn), copper (Cu) and lead corrosion caused by high chloride (Cl) deposition, and corrosion of glass representative of medieval stained glass windows.

9. Risk maps are similar to damage maps, but they are used when the function only gives a relative measure of damage, for example by a risk index. They comprise decay of indoor wooden objects due to humidity shocks and outdoor wooden structures by fungal growth, and to moisture content of spruce wood, sandstone and brick. For individual metals, risk maps are not necessary, since damage maps exist expressing the damage in μm. For metals, however, a multiple-risk map has been produced (see below).

III. GUIDELINES FOR ADAPTATION STRATEGIES

10. The aim of the guidelines for adaptation strategies is to disseminate information on climate change effects and the most appropriate adaptation strategies for Europe's cultural heritage managers. The guidelines complement the vulnerability atlas. They include chapters on climate change and cultural heritage, heritage structures and infrastructure, principles of mitigation, principles of adaptation, future research orientations and a summary of recommendations. Specific conclusions and recommendations for individual materials include outdoor stone and brick, wood and metals. The conclusions for stone, brick and wood are summarized in this section while the conclusions for metals are elaborated in detail in the subsequent sections.

11. When classifying stone degradation, two key properties should be considered: chemical composition and porosity. Based on this, the following damage processes have been considered: surface recession, blackening, thermoclastism, frost, salt weathering and biodeterioration.

12. Surface recession refers to the chemical attack induced by the effect of clean and acid rain and the dry deposition of gaseous pollutants. Maps produced for the twenty-first century showed a general increase in surface recession in northern Europe and a decrease in southern Europe.

13. Deposits of soot disfigure buildings and cause blackening. The general degree of soiling can be directly related to the concentration of particulate matter in air. The distribution of the blackening pattern is equally important. There is a strong negative public reaction to vertical rain-washed streaks. Blackening features, which obscure or conflict with architectural form, induce the most adverse reaction.

14. Thermoclastism refers to the process of differential thermal expansion and contraction of surface mineral grains and interstitial salt deposits, such as nitrates, in response to long- and short-term temperature fluctuations at the material surface. Because heat conduction coefficients of stones are very low, a high temperature gradient occurs within the surface layer, leading to

microfracture development and possibly exfoliation. The data demonstrated that the Mediterranean area will continue to experience the highest level of risk from thermal stress.

15. The effect of the freeze-thaw cycle is often the most evident sign of climate weathering in cooler regions. Frost damage is caused when wet stone freezes and the associated volume change causes the outer layers to shatter. A reduction in frost effects is likely in the future in temperate Europe.

16. Salts present in porous materials are a major contributor to the weathering process. The most obvious change is an increase in the frequency of transition across the critical relative humidity point for sodium chloride (75.5%). Evidence suggested that this was likely to be most prevalent in an area that stretches from northern Spain to the United Kingdom and back across France and Germany into central Europe. In this area, there are many Gothic buildings constructed in softer porous stones.

17. Building materials are prone to colonization by organisms, which are linked to environmental conditions. It was predicted that climate change in Europe will have a considerable effect on this colonization.

18. Historic wooden structures and objects deteriorate by two mechanisms: (a) mechanical damage due to climatic variations, mainly in ambient relative humidity; and (b) biological attack by wood-destroying fungi.

19. Dimensional change in wood leads to stresses within the material, which can cause significant physical damage. If a relatively humid wood is desiccated and restrained from natural shrinkage, the materials will experience an increase in tension. Humidity shocks in Europe will remain an important agent of deterioration for historic wooden artefacts. The risk will generally increase, except in the very northern part of Europe.

20. Most fungal problems in historic buildings occur in the presence of excess moisture, with the two most important climatic parameters being precipitation and temperature. The risk for fungal attack will increase in the north and east of Europe and will decrease in south and west of Europe.

IV. COMBINED EFFECTS OF CLIMATE CHANGE AND AIR POLLUTION ON METAL CORROSION

21. Important causes of the atmospheric corrosion of metals can be grouped into the following categories: climatic parameters, gaseous air pollutants, particulate air pollutants and

acid rain. In reality, the effects are combined in a complex way described by the dose-response functions developed within ICP Materials and other exposure programmes. For example, the dose-response function for Zn in the sulphur dioxide-dominating situation developed by ICP Materials is

$$ML = 1.4\,[SO_2]^{0.22}\, e^{0.018Rh}\, e^{f(T)} t^{0.85} + 0.029\,Rain[H^+]\,t\,,$$

where ML is the mass loss in g m^{-2}, $[SO_2]$ is the sulphur dioxide concentration in µg m^{-3}, Rh is the relative humidity in per cent, f(T) is a function of temperature in °C equal to 0.062(T-10) when T is lower than 10°C and -0.021(T-10) when T is higher than 10°C, t is the time in years, Rain is the amount of annual precipitation in mm, and [H+] is the hydrogen ion concentration in precipitation in mg l^{-1}.

22. Two main effects were considered: (a) the combined effect of temperature and SO_2 pollution, illustrated for carbon steel; and (b) the combined effect of temperature and Cl deposition, illustrated for Zn. These two effects were also combined in a multiple-risk map.

A. The combined effect of temperature and sulphur dioxide pollution

23. Temperature and relative humidity act in combination to determine the wetness conditions on a metal surface. When the surface is sufficiently wet, pollutants may dissolve in the surface layer and act as corrosive agents. Therefore, climate and pollution are dependent and should be considered together. Figure 2 shows the most common temperature dependence for metals.

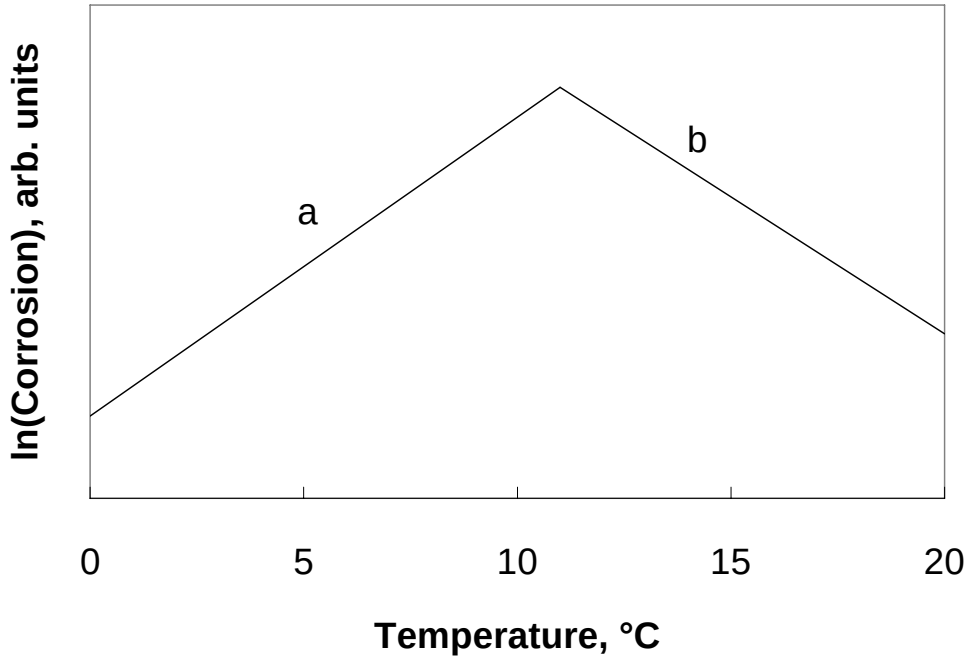

Figure 2. Schematic representation of the observed annual temperature dependence for many materials. Line a: an increase of corrosion with temperature due to increase of time of wetness. Line b: a decrease of corrosion with temperature due to fast evaporation of moisture after rain or condensation periods.

24. The temperature dependence illustrated in figure 2 is exemplified in figure 3 by selecting the three cells indicated in figure 1. These grid cells are denoted “Riga”, “London” and “Rome” for ease of identification, since these cities are located within the selected grids cell. All values are grid cell averages. The results showed that if the pollution situation remained unchanged, the effect of global climate change would be significant. The corrosion in the London grid remained high since the temperature changed from about 8°C to about 12°C. An increasing temperature for “Rome”, from about 11°C to 17°C, was a typical example of how drying out the surface reduces the corrosion rate (line b in figure 2). The temperature was increasing also for “Riga”, from 2°C to 9°C, but in this case the corrosion rate increased (line a in figure 2).

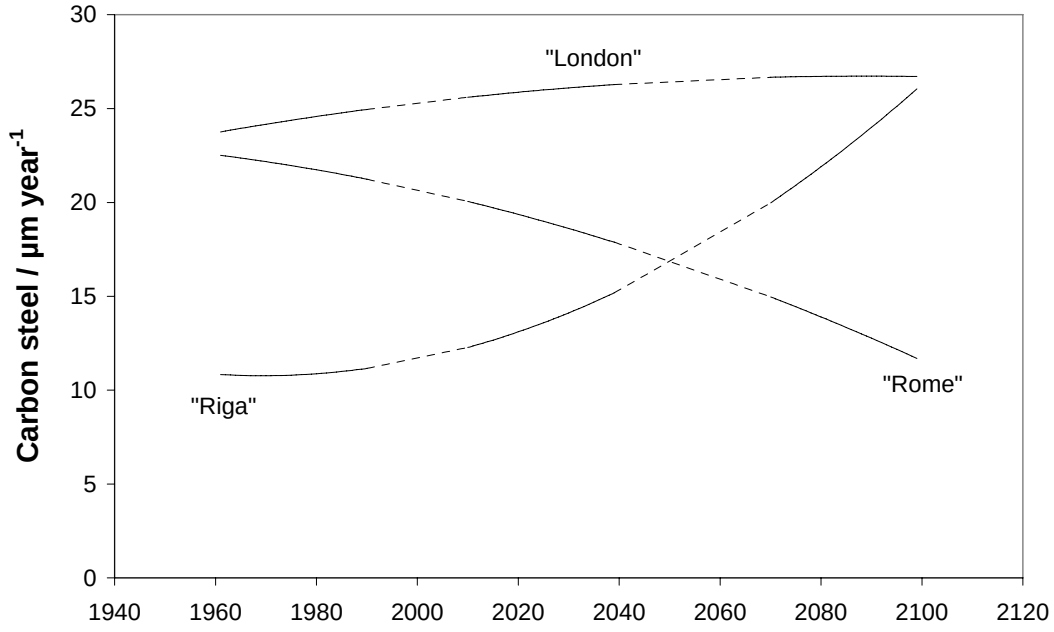

Figure 3. Calculated corrosion of carbon steel due to SO_2 assuming a constant SO_2 level of 10 µg m^{-3}. Results for three grid cells are given (“Riga”, “London” and “Rome“). Solid lines are shown for the periods with available data (1961–1990, 2010–2030 and 2070–2099).

B. The combined effect of temperature and chloride deposition

25. The corrosion rate of most metals is strongly affected by the Cl concentration on the surface. Chlorides have hygroscopic properties and thus contribute to the creation of an electrolyte layer. This leads to a prolongation of the periods when the surface is wet, even at high temperatures. Therefore, the temperature decrease observed in figure 2.b is not observed for the

Cl effect. Instead, the corrosion continues to increase with temperature also above 10°C (figure 4). In addition, chlorides are corrosive and can cause pitting corrosion. The highest observed corrosion rates in the world today, with the exception of certain aggressive industrial atmospheres, can be found at warm marine sites in subtropical and tropical regions.

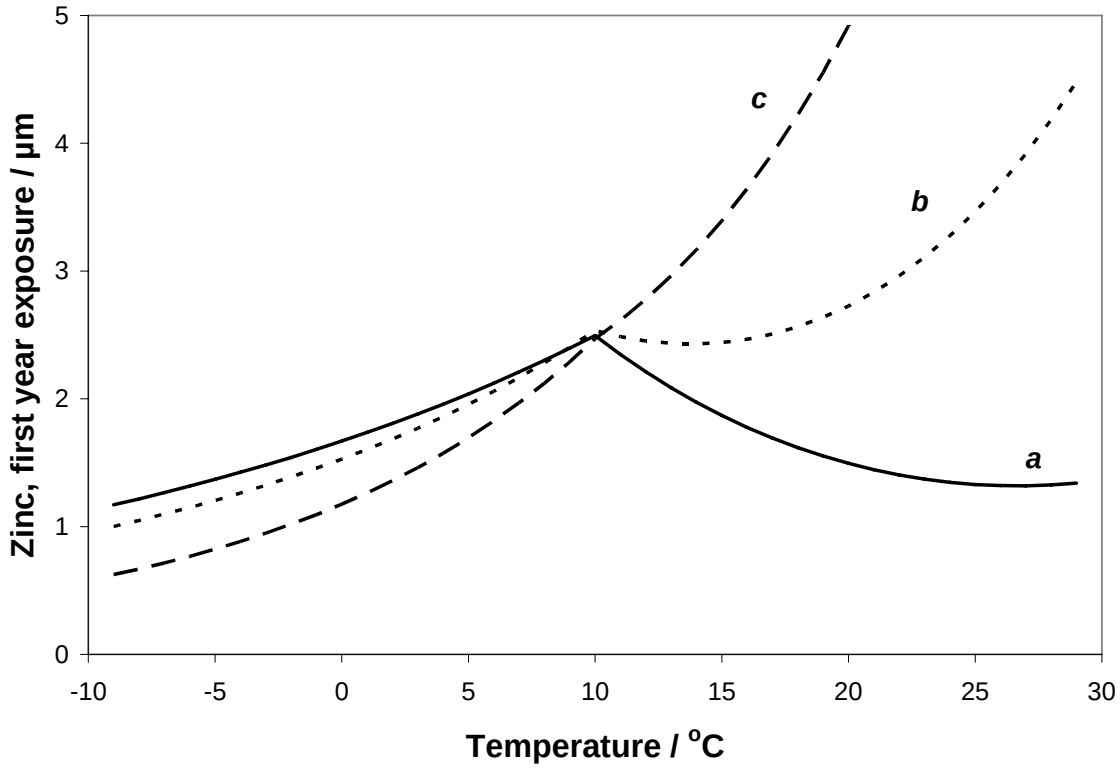

Figure 4. Calculated corrosion of Zn as function of the temperature using different parameter values. Line a: SO_2 = 40 µg m^{-3}, Cl = 3 mg m^{-2} day^{-1}. Line b: SO_2 = 20 µg m^{-3} and Cl = 60 mg m^{-2} day^{-1}. Line c: SO_2 = 1 µg m^{-3} and Cl = 300 mg m^{-2} day^{-1}.

26. The dependence for Cl deposition is given for Zn in figure 4 by selecting the same three grid cells in figure 3. The deposition level chosen to illustrate the effects (300 mg m^{-2} day^{-1}) is relatively high, but can occur within hundreds of metres from the seashore or in areas where roads are salted. Relative humidity is expected to decrease when temperature increases. For carbon steel, the effect of relative humidity and temperature is of equal importance and the decreasing relative humidity tends to balance the increasing temperature. For Zn, the temperature is dominating, and an increasing corrosion due to increasing temperature is observed everywhere.

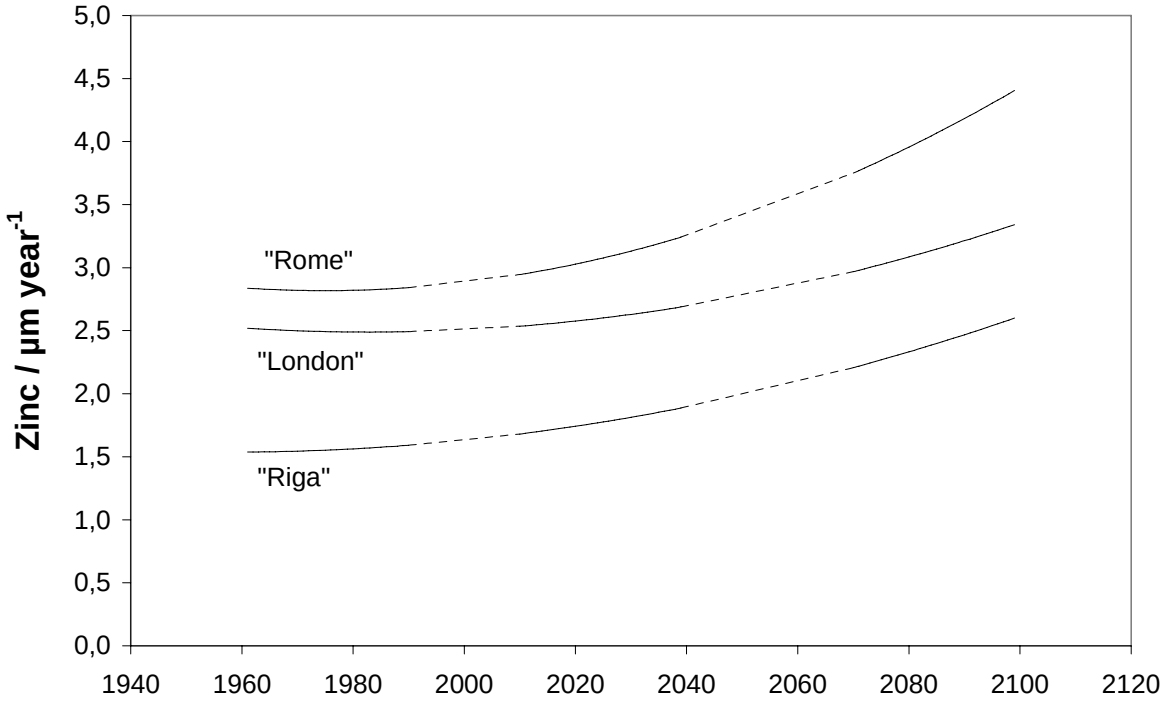

Figure 5. Calculated corrosion of Zn due to Cl deposition assuming a constant Cl deposition of 300 mg m-2 day-1 for three grid cells ("Riga", "London" and "Rome").

C. Multiple-risk map for metals

27. Carbon steel has been used to illustrate the combined effect of temperature and SO_2 pollution and is a very good indicator of iron and bronze corrosion in environments dominated by acidifying pollutants. Zn has been used to illustrate the combined effect of temperature and Cl deposition. A multiple-risk map for metals in general can be obtained by synthesizing the two effects. The map will be valid for metals in general since for all metals SO_2 pollution and Cl deposition are the two most important factors governing corrosion. The purpose of the map is to show areas where corrosion of metals can increase or decrease due to future climate changes, but not to serve as a tool for estimating corrosion attack in individual areas. If the corrosion value needs to be determined, individual maps for specific metals should be used.

28. The combination of maps for individual metals is based on the standard ISO[2] 9223 "Corrosion of metals and alloys–Corrosivity of atmospheres–Classification". The standard is broadly applied and has been adopted in other national and international standards. The purpose of ISO 9223 is to describe how to obtain a corrosivity category for carbon steel, Zn, Cu or

[2] International Organization for Standardization.

aluminium. The corrosivity category is a technical characteristic that provides a basis for the selection of materials and protective measures. It is labelled from C1 to C5, where C1 and C5 correspond to a very low and very high corrosivity, respectively. The table below shows the corrosivity categories for the different metals. The highest category (C5) specifies upper limits. Measured values above these limits have been detected in the field but are beyond the scope of the present standard.

ISO 9223 Corrosivity categories for carbon steel, Zn, Cu and aluminium based on corrosion rates

Corrosivity	Category	Steel µm year^{-1}	Zinc µm year^{-1}	Copper µm year^{-1}	Aluminium g m^{-2} year^{-1}
Very low	C1	≤1.3	≤0.1	≤0.1	negligible
Low	C2	1.3–25	0.1–0.7	0.1–0.6	≤0.6
Medium	C3	25–50	0.7–2.1	0.6–1.3	0.6–2
High	C4	50–80	2.1–4.2	1.3–2.8	2–5
Very high	C5	80–200	4.2–8.4	2.8–5.6	5–10

29. Based on the table above, the two maps of carbon steel and Zn have been combined by use of corrosivity category (C1–C5) for Zn in coastal areas, and use the corrosivity category (C1–C5) for carbon steel in inland areas. In order to make the transition from coastal to inland areas less abrupt an intermediate case was also added by using the corrosivity category (C1–C5) for Zn in near-costal areas, but calculated based on a lower Cl deposition rate than for the original Zn map. This intermediate deposition rate was determined from modelled values of Cl deposition, depending on the distance from the coastline.

30. Coastal areas were defined as the grid (50 km × 50 km) intersecting the coastline while near-costal areas were defined as a one-grid thick zone in between the coastal and inland areas. The Cl deposition levels used were 300 mg m^{-2} day^{-1} for coastal areas and 60 mg m^{-2} day^{-1} for near-coastal areas.

31. The multiple-risk map for metals shown in figure 5 is a difference map showing the change in corrosivity category from the recent past (1961–1990) to the far future (2070–2099). For example, an increase of 0.5 in corrosivity category could mean an increase from lower C3 to middle C3 (25 to 37.5 µm for carbon steel or 0.7 to 0.9 µm for Zn) or from middle C5 to upper C5 (140 to 200 µm for carbon steel or 6.3 to 8.4 µm for Zn). In inland areas, the temperature maximum (see figure 2) resulted in an increase of corrosion in northern Europe and a decrease in southern Europe. In coastal areas, corrosion was expected to increase everywhere due to the increased temperature.

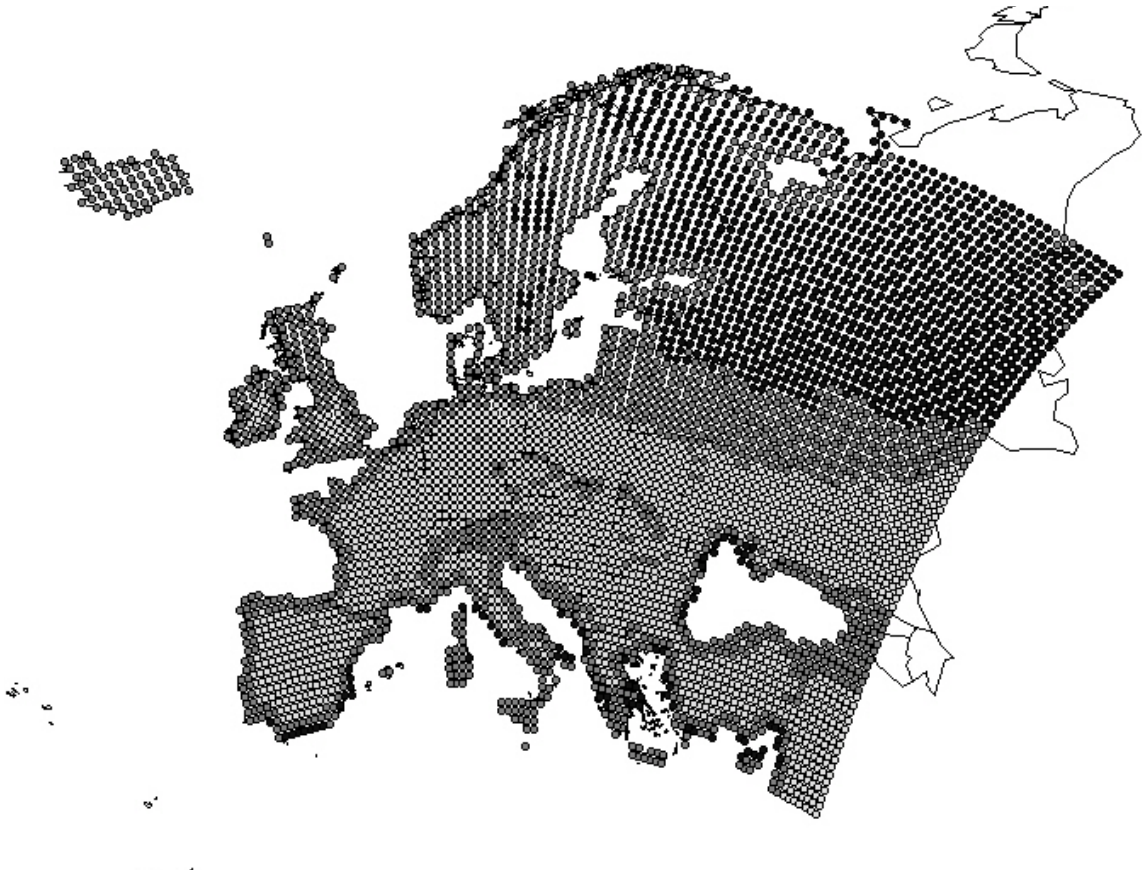

Figure 6. Multiple-difference corrosivity map for metals showing areas with decreased (: –0.5 to 0.0), increased (•: 0.0 to 0.5) and very increased (●: 0.5 to 1.0) corrosivity category.

V. CONCLUSIONS

32. The degradation of materials and cultural heritage caused by climate change has not yet been dealt with in international programmes and has so far not been in focus compared to other effects of climate change. The EU project NOAHs ARK was the first international project to deal with climate change impact on historic buildings and cultural landscapes. Dose-response functions from ICP Materials provided essential input to the project.

33. The vulnerability atlas provides maps on a European scale. It is a tool for identifying areas and effects of interest to be mostly affected by climate change in the future, and is therefore useful for policymakers at the national and international levels.

34. The guidelines for adaptation are a complement to the vulnerability atlas. It gives overall strategies useful to national policymakers, but also gives guiding principles for heritage managers, useful on a local scale, on how to adapt to the increased stresses on our cultural heritage due to climate change.

35. The combined effects of climate and pollution have been exemplified for carbon steel and Zn and combined in a multiple-difference risk map for metals. This map shows that the corrosion to metals is expected to increase in coastal areas due to the combined effect of temperature and Cl deposition. It also shows that the corrosion to metals in areas affected by SO_2 pollution is expected to increase in the northern part of Europe and to decrease in the southern part of Europe.

36. Climate and pollution are acting together in a complex way, resulting in corrosion and degradation of materials. Even if the greatest effects of reducing air pollutants, regarding the degradation of materials, have already been observed in Europe, further reducing air pollutants is one of the more effective ways of compensating for increased risk of corrosion due to climate change. The effects of global climate change are closely related to local changes in air pollution trends. Future revisions and formulations of air quality directives aimed at the protection of cultural heritage and the built environment should consider this.
